ATOM-PROBE TOMOGRAPHIC ANALYSES OF ALLENDE AND SYNTHETIC NANODIAMONDS.

P. R. Heck[1,2], M. J. Pellin[2,3,4,6], A. M. Davis[1,2,3,6], D. Isheim[7], D. N. Seidman[7], J. Hiller[4], A. Mane[8], J. Elam[8], M. R. Savina[2,4], O. Auciello[4,5], T. Stephan[1,2,3,4], F. J. Stadermann[9,10], J. Lewis[9,10], X. Zhao[9,10], T. L. Daulton[10,11], and C. Floss[9,10]. [1]Robert A. Pritzker Center for Meteoritics and Polar Studies, Dept. of Geology, The Field Museum, Chicago, IL. E-mail: prheck@fieldmuseum.org. [2]Chicago Center for Cosmochemistry, [3]Dept. of the Geophysical Sciences, Univ. of Chicago, Chicago, IL. [4]Materials Science Division and [5]Center for Nanoscale Materials Argonne National Laboratory, Argonne, IL. [6]Enrico Fermi Institute, Univ. of Chicago, Chicago, IL. [7]Northwestern Univ. Center for Atom-Probe Tomography, Dept. of Materials Science & Engineering, Northwestern Univ., Evanston, IL. [8]Energy Systems Division, Argonne National Laboratory, Argonne, IL. [9]Laboratory for Space Sciences, [10]Physics Dept., [11]Center for Materials Innovation, Wash. Univ., St. Louis, MO.

Introduction & Motivation: Nanodiamond is the most abundant and the first discovered phase thought to be presolar in unequilibrated meteorites, based on highly anomalous Xe isotopes [1] and small Ba, Pd, and Te isotopic anomalies [2,3,4]. In contrast, the $^{12}C/^{13}C$ and $^{14}N/^{15}N$ ratios are close to solar [5,6]. This observation supports another hypothesis that most of the diamonds formed in the Solar System [7]. Stroud et al. [8] observed that nanodiamonds in meteoritic acid residues are associated with glassy C. This was explained by the transformation of organics to nanodiamonds and glassy C by supernova shockwaves in the interstellar medium [8]. The different hypotheses reflect that nanodiamonds are still one of the least understood refractory phases in meteorites. Because of their small sizes (avg. diameter ~3 nm [9]) it has not been possible to analyze the isotopic compositions of individual nanodiamonds, which would help to constrain their origins. It is not known, therefore, if some of the diamonds have anomalous $^{12}C/^{13}C$ ratios. Atom-probe tomography (APT) is currently the only technique that has the spatial resolution and sensitivity to analyze isotopes of individual nanoparticles [10]. During the last three years, we developed sample preparation techniques and analytical protocols to analyze individual nanodiamonds with APT. First results on mass spectrometric APT analyses of individual nanodiamonds were presented recently [11–13]. Here, we report on our progress toward determining $^{12}C/^{13}C$ ratios of individual nanodiamonds.

Samples & Methods: We used aliquots of the Allende DM nanodiamond acid residue [14]. Detonation and ultrananocrystalline diamond (UNCD) films served as synthetic analytical standards. Sample preparation is most critical for successful APT analysis. Previously, most samples failed mechanically during APT analysis. Our new sample preparation approach aims at improving sample stability by minimizing weak interfaces. It consists of direct deposition of a nanodiamond residue onto presharpened and flat-top Si microtips. To enhance sample stability we filled open pore space with atomic layer deposition of Al_2O_3 and W [15]. A protective Co layer was sputter-deposited onto the flat-top microtips before shaping them by focused ion-beam milling. Samples were analyzed with a Cameca Instruments LEAP4000XSi tomograph, equipped with a focused picosecond ultraviolet (wavelength = 355 nm) laser [10].

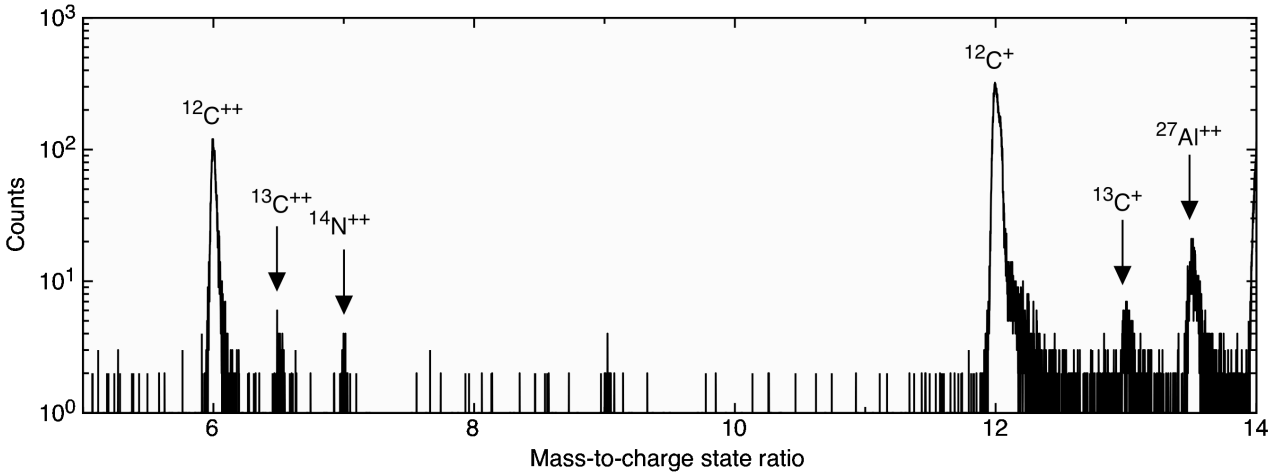

Figure 1. Time-of-flight mass spectrum of Allende DM nanodiamond sample integrated for one microtip. Note the sharp peaks and low background. The mass-to-charge state ratio range was selected to show peaks of C ions.

Results & Discussion: The new sample preparation approach resulted in highly improved sample stability. Analyses of both types of tips are usually stopped manually after the exposed Si tip itself completely fills the field-of-view of the detector. Time-of-flight mass spectra (Fig. 1) of both types usually exhibit sharp peaks and low background noise, which permits us integrate peaks of ions of ^{12}C, ^{13}C, ^{27}Al, ^{28}Si, ^{29}Si, ^{30}Si. Subsequent tomographic reconstructions reveal the differences between the two microtip types: The flat-top microtips show a thick, rather homogeneous, low-contrast layer of nanodiamond sandwiched between the Si flat-top and the sharpened Co cap at the tip apex. Alternatively, the presharpened Si microtips exhibit a very heterogeneous distribution of C on their surfaces, corresponding to individual and clusters of nanodiamonds. We, therefore, prepared and analyzed more samples on presharpened microtips.

We determined preliminary raw peak ratios of $^{12}C^+/^{13}C^+$ for integrated tips of synthetic and Allende nanodiamonds, in addition to a small number of regions of interest (ROIs) in Allende samples. The ROIs were of the same volume as average Allende nanodiamonds and were centered on C concentration hotspots, Fig. 2. The ROIs contain ~1000 detected C atoms, corresponding to ~2000 C atoms with the LEAP's 50% yield, the same number that is expected for individual nanodiamonds. We found the $^{12}C^+/^{13}C^+$ ratios of the ROIs and the integrated tips to be identical, within experimental uncertainties. All these ratios are uncorrected for any instrumental bias. We will systematically investigate the instrumental bias by analyzing a suite of synthetic, UNCD films standards with varying C isotopic compositions. Once we can correct for instrumental bias, we will be able to determine C isotope ratios of individual nanodiamonds. Analyzing a large number of individual nanodiamonds will provide the distribution of $^{12}C/^{13}C$ ratios and will help to constrain their origins.

References: [1] Lewis R. S. et al. (1987) *Nature 326:*160–162. [2] Lewis R. S. et al. 1991, *LPSC* 22: 807 [3] Richter S. et al. (1998) *Nature* 391:261–263. [4] Maas R. et al. (2001) *MAPS* 36:849–858. [5] Russell S. S. et al. (1996), *MAPS* 31:343. [6] Marty B. et al. (2011) *Science* 332:1533–1536. [7] Dai Z. R. et al. (2002) *Nature* 418:157–159. [8] Stroud R. M. et al. (2011) *ApJL* 738:L27. [9] Daulton T. L. et al. (1996) *GCA* 60:4853– 4872 [10] Seidman D. N. and Stiller K. (2009) *MRS Bull. 34*, 717–721. [11] Heck P. R. et al. (2011) *LPS XLII*, Abstr. #2112. [12] Stadermann F. J. et al. (2011) *LPS XLII*, Abstr. #2134. [13] Heck et al. (2011) *MAPS* 46:A90. [14] Lewis R. S. et al. (1989) *Nature* 339:117–121. [15] Elam J. W. et al. (2006) *Appl. Phys. Lett. 89:*053124.

Acknowledgements: We thank R. S. Lewis for providing the meteoritic nanodiamond sample, K. B. Knight for providing synthetic detonation nanodiamonds, and J. Pearson for sputter coating. Funding is provided by the NASA Cosmochemistry Program and the Tawani Foundation. The LEAP tomograph at NUCAPT was purchased and upgraded with funding from NSF-MRI and ONR-DURIP grants. Part of the research was performed at Argonne National Laboratory, a U.S. DOE Office of Science Laboratory operated under Contract No. DE-AC02-06CH11357 by UChicago Argonne, LLC.

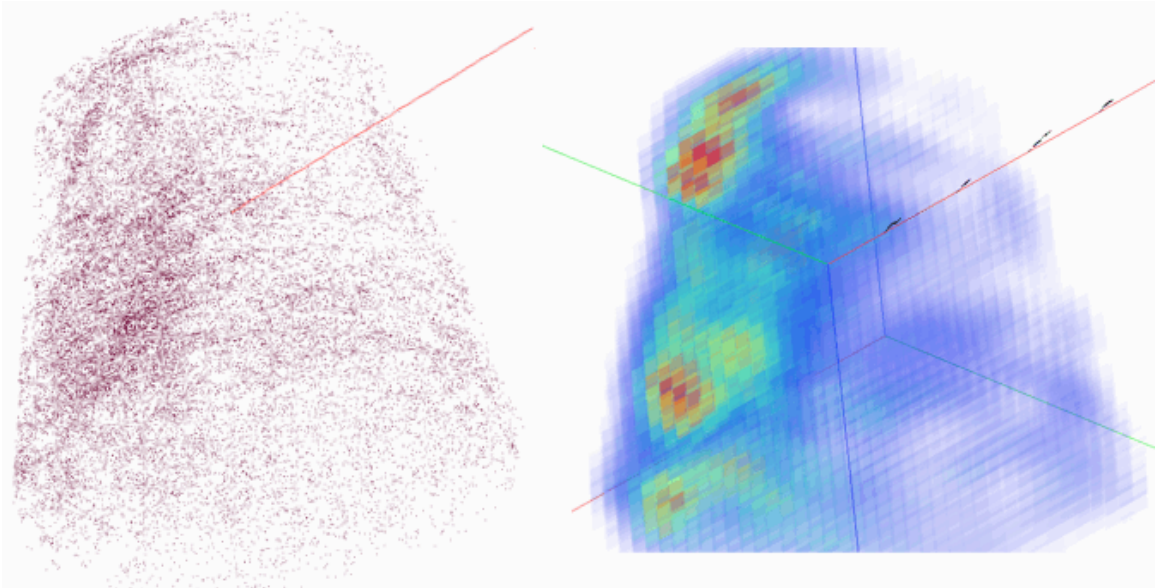

Figure 2. Left-hand side: Tomographic reconstruction of Allende DM sample on the surface of a presharpened microtip. Only C atoms are shown. Right-hand side: Color-coded concentration C hotspots on the sample.